JJMIE

Volume 9 Number 2, April.2015
ISSN 1995-6665
Pages 121 - 128

Jordan Journal of Mechanical and Industrial Engineering

Corrosion Characteristics of Basalt Short Fiber Reinforced with Al-7075 Metal Matrix Composites

Ezhil Vannan * a, Paul Vizhian b

[a] *Professor, Department of Mechanical Engineering, H.K.B.K College of Engineering, Nagawara, Visvesvaraya Technological University, Bangalore, India.*
[b] *Professor, Department of Mechanical Engineering, University Visveswarya College of Engineering,K.R. Circle, Bangalore University, Bangalore, India*

Received 17 June 2014 *Accepted 22 March 2015*

Abstract

This paper reports a study of the corrosion characteristics of Al 7075/ basalt short fiber metal matrix composites in 1 M HCl solution at room temperature as a function of percentage of reinforcement. The percentage of reinforcement was varied from 2.5 to 10 wt.% in steps of 2.5% and the composites were prepared by the liquid metallurgy technique. The weight loss method was used to determine the corrosion rate. The durations of the tests ranged from 24 to 96 hrs in the steps of 24 hrs. Both the unreinforced matrix alloy and the composites were subjected to identical test conditions to study the influence of the reinforcement on Al 7075/ basalt corrosion behavior. The corrosion rates of both the unreinforced matrix alloy and the composites decreased with the exposure time. The corrosion rate of MMCs was lower than that of matrix Al 7075 alloy under the corrosive atmosphere. Scanning Electron Microscopy (SEM) was used to study the corroded surface of the specimens.

© 2015 Jordan Journal of Mechanical and Industrial Engineering. All rights reserved

Keywords: *Metal Matrix Composite; Aluminium Alloy, Basalt Fiber; Corrosion*.

1. Introduction

In the recent years, there has been a great interest in searching for new materials, which offers designer many added benefits in designing the components for automobile and aircraft industry through Metal Matrix Composites (MMCs). Aluminium based MMCs offer designers many added benefits, as they are particularly suited for applications requiring good strength at high temperatures, good structural rigidity, dimensional stability, and lightweight [1-4]. The trend is toward safe usage of the MMCs parts in the automobile engine, particularly at high temperature and pressure environments [5, 6]. Fiber reinforced MMCs that have been most popular over the last two decades have attracted considerable attentions [7-10]. Fiber reinforced MMCs find their utilization in the rapidly broadening field of application. They have been widely used in many industries such as aircraft, aerospace, automobiles, ships and civil constructions. These materials maintain good strength at high temperature, good structural rigidity, dimensional stability and light weight [11-13]. Reinforced Al MMCs find Potential applications in several thermal environments, especially in the automobile engine parts, such as drive shafts, cylinders, pistons, and brake rotors. Al-based MMCs which are used in automobile engine parts normally encounter acidic environments containing chloride, sulphiate and nitrate radicals, in addition to exhaust gases like CO_2, CO and NO_2. MMCs used at high temperatures should have good mechanical properties and resistance to chemical degradation in air and acidic environments [14]. High strength aluminum alloys, such as 7075, are widely used in aircraft structures, aerospace and automobiles due to their high strength-to-weight ratio, machinability, superior wear resistance, improved elevated temperatures tensile and fatigue strengths and low cost. However, due to their compositions, these alloys are susceptible to corrosion. Corrosion is a major concern involving the structural integrity of aircraft structures and automobile components. Considerable attention is focused on aluminum based metal matrix reinforced with high strength and high modulus ceramic reinforcements because of their superior properties [15, 16]. For high temperature applications, it is essential to have a thorough understanding of the corrosion behavior of the aluminium composites. Reported literature [17–19] indicates that the addition of SiC particles do not appear to improve corrosion resistance of some aluminium alloys because pits were found to be more numerous on the composites than on the unreinforced alloys although they were comparatively smaller and shallower than those on the unreinforced alloy.

* Corresponding author. e-mail: ezhilsil@yahoo.co.in.

As far as we know, although many researchers have worked on corrosion characteristics of fiber reinforced metal matrix composites, no concrete investigation has been made on basalt fiber reinforced with aluminum alloy 7075 metal matrix composites. The present paper focuses on the corrosion characteristics of Al 7075/ basalt short fiber metal matrix composites.

2. Materials and Methods

2.1. Materials

The Al and basalt short fiber used as the MMCs in the present study are obtained from commercial ingots with correct chemical composition. The presence of these elements have been confirmed by SEM / EDS spectra. The Energy Dispersive Spectroscopy [EDS] spectrum also shows the presence of impurities such as iron and basalt short fiber in traces. The alloy is found to be pollution free in the foundry. Because of its low energy requirements and excellent machinability, it is expected to reduce the production time and lengthen tool life during its fabrication process. The matrix alloy used in the present investigation was Al 7075 alloy, which has basalt short fiber reinforcement; the chemical composition is shown in Tables 1 and 2 [20].

Table 1. Chemical composition of Al alloy- Weight percentage

Element	Si	Fe	Cu	Mn	Mg	Cr	Zn	Ti	Al
%	0.4	0.5	1.6	0.3	2.5	0.15	5.5	0.2	Bal

Table 2. Properties of matrix alloy

Density	2.7 gm/cc
Young’s modulus	75 GPa
UTS	170 MPa
Ductility	13.5 %
Melting temperature	650° C

2.2. Reinforcement

The basalt fiber was made from naturally occurring basalt rock in the Washington State area, USA. The basalt short fiber, used as reinforcement in the present investigation, has been purchased from a mineralogical research company. The chemical composition of the fibers is determined by the native basalt rock used as a raw material, whose main composition is shown in Table 3 [21].

Table 3. Chemical composition of short basalt fiber

Element	SiO_2	Al_2O_3	Fe_2O_3	MgO	CaO	Na_2O	K_2O	TiO_2	MnO
%	69.51	14.18	3.92	2.41	5.62	2.74	1.01	0.55	.04

The fiber was produced in a prototype device. The basalt rock was melted in a platinum-rhodium crucible at 1250±1350°C. The fiber was drawn from the melt through a fiber in the crucible and wound onto a rotating drum continuously. Fibers in roving form were bundled and cut into short fibers of uniform length about 0.5 to1 mm in size by constant-length cutter. The short Basalt short fiber was cleaned in distilled water and dried at 90°C.

2.3. Composite Preparation

The liquid metallurgy route using vortex techniqueis employed to prepare the composites. The weight percentage of the basalt short fiber added was 2.5, 5, 7.5 and 10% to prepare the MMCs. A muffle furnace was used to preheat the copper coated basalt short fiber to a temperature of 500°C and maintained at that temperature till it was introduced into the Al alloying elements melt. The preheating of the reinforcement is necessary in order to reduce the temperature gradient and to improve wetting between the molten metal and the basal short fiber. Known quantities of these metals ingots were pickled in 10% NaOH solution at room temperature for ten minutes. Pickling was done to remove the surface impurities. The smut formed was removed by immersing the ingots for one minute in a mixture of 1:1 volume/volume of nitric acid and water followed by washing in methanol. These cleaned ingots after drying in the air were loaded into different alumina crucibles. These crucibles kept in composites furnace, which were setting metals respected melting temperature. The melts were super-heated and maintained at that temperature. The temperatures were recorded using a chromel-alumel thermocouple. The molten metals were then degassed using purified nitrogen gas. The purification process with commercially pure nitrogen was carried out by passing the gas through an assembly of chemicals arranged in a row (concentrated sulphuric acid and anhydrous calcium chloride, etc.) at the rate of 1000 cc/ minute for about 8 minutes. A stainless steel impeller or stirrer coated with alumina was used to stir the molten metal and create a vortex. The impeller used for stirring was of centrifugal type with three blades welded at 45° inclination and 120° apart. The stirrer was rotated at a speed of 500 rpm and a vortex was created in the melt. The depth of immersion of the impeller was approximately one third the height of the molten metal above the bottom of the crucible. The reinforcing basalt short fiber, which was preheated in the muffle furnace, was introduced into the vortex at the rate of 120 gm/min. Stirring was continued until interface interactions between the basalt short fiber and the matrix promoted wetting. Then the melt was degassed using pure nitrogen for about 3-4 minutes and after reheating to super heat temperature (540°C), it was poured into the pre heated lower half die of the hydraulic press. The top die was brought down to solidify the composite by applying a pressure of 100 kg/sq.cm. Both the lower die and the upper dies were preheated to 280°C, before the melt was poured into it. The pressure applied enables uniform distribution of the basalt short fiber in the developed composite [22].

2.4. Specimen Preparation

Cylindrical specimens of diameter 15mm and thickness 5mm were machined from castings of the composites and of the unreinforced alloy using an abrasive cutting wheel. Before corrosion testing, the specimen surfaces were ground using 240, 320, 400 and 600 SiC paper, in this order, using distilled water as a lubricant and a coolant in order to obtain a smooth and identical surface finish on all the specimens [23]. The specimen were then washed in distilled water, followed by acetone, and then allowed to dry thoroughly [24]. Before corrosion testing, each test specimen was etched with killer's agent and examined under optimal microscope. They were finally weighed to an accuracy of three decimal places. This same cleaning procedure was used before each weighing at each stage of the corrosion test.

2.5. Corrosion Test

The corrosion test was conducted at room temperature (27°C) using conventional corrosion rate measurement according to ASTM G1-03 and ASTM G31-72 [25, 26]. The area of the specimen, subjected to corrosion, was calculated before performing corrosion test using the following equation (according to ASTM G31–72):

$$A = (\pi / 2(D^2 - d^2)) + t\pi D + t\pi d, \quad (1)$$

where t is thickness, D is diameter of the specimen, and d is diameter of the mounting hole. The corrodents used for the tests were 1M hydrochloric acid. Small cylindrical discs of 15mm diameter and 5mm thickness were polished using emery paper in order to obtain a smooth and identical surface finish on all specimens, and then washed in distilled water, followed by acetone, and then allowed to dry thoroughly [27]. They were finally weighed accurately to an accuracy of three decimal digits. The initially weighted specimens were immersed in the corrosive environment and taken out at 24 h intervals for testing up to 96 hr. To avoid crevice corrosion, the specimens were suspended in the solution with a plastic string. The specimens were exposed to the test solution for several hours up to 96 hr. The corroded surface was removed by immersing the specimen on 100 mg ammonium per sulphate for 5 min. The cleaned specimens were dried and weighed to an accuracy of three decimal digits. After drying thoroughly, the specimens was weighed again and then placed in a dessicator to prevent corrosion. Weight loss was calculated and converted into corrosion rate and expressed in mils penetration per year (myp). The corrosion rate was calculated and compared with other reinforcements. The Corrosion Rate (CR), from the mass loss, was calculated (according to ASTM Standard [28, 29] using the following equation:

$$\text{CR} = (K \times W) / A \times T \times D) \quad (2)$$

where CR is corrosion rate (mm/year), K is a constant equal to 8.76×10^4, T is time of exposure in hours to the nearest 0.01 hour, A is area in cm^2, $W$is mass loss in grams, and D is density in g/cm^3. The microstructure was examined using CETI optical microscope and the corroded surface was studied using SEM Model Quanta FEG 250. Tables 4 and 5 show the average corrosion rates of Al7075 as well as Al7075/basalt fiber MMCs; the average is of 10 samples.

Table 4. The average corrosion rates of Al7075

Exposure duration (hr)	Area of specimen (mm^2)	Average corrosion rate (mm/year)
24	274.89	0.08
48	274.89	0.045
72	274.89	0.032
96	274.89	0.024

Table 5. The average corrosion rates of Al7075/Basalt fiber MMCs

Basalt fiber (Wt. %)	Exposure duration (hr)	Average corrosion rate (mm/year)
2.5	24	0.096
	48	0.054
	72	0.038
	96	0.025
5	24	0.118
	48	0.062
	72	0.042
	96	0.032
7.5	24	0.13
	48	0.752
	72	0.573
	96	0.39
10	24	0.158
	48	0.089
	72	0.058
	96	0.040

3. Results and Discussion

3.1. Effect of Test Duration of Exposure to Corrodent

Figure 1 shows the plot of corrosion rate (in mpy) of the as cast and the composites in 1M HCl solution against exposure time (in hrs). It can be seen that in every case, there is a decrease in the corrosion rate with an increase in duration of the exposure to the corrodent, implying that the corrosion resistance of the material tested increases as the exposure time is increased. This eliminates the possibility of hydrogen bubbles clinging on to the surface of the specimen and forming a permanent layer affecting the corrosion process. The phenomenon of gradually decreasing corrosion rate indicates the possible passivation of the matrix alloy. Visual inspection of the specimens after the corrosion tests revealed the presence of black-film covering the surface, which might have retarded the corrosion rate. De Salazar [30] explained that the protective black film consists of hydrogen hydroxy chloride, which retards the forward reaction. Castleet.al [31] pointed out that the black film consists of aluminium hydroxide compound. This layer protects further corrosion in acid media. But the exact chemical nature of such protective film is still not determined.

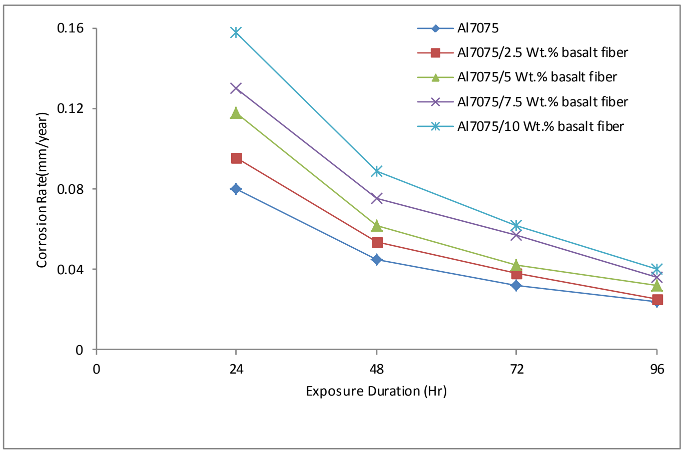

Figure 1. Corrosion rate of unreinforced matrix alloy and composites in 1 M HCl solution against exposure time

3.2. Effect of Basalt Short Fiber Content

From Figure 1, it is apparent that for both the unreinforced matrix and composite, there is a trend of decreasing corrosion rate with increase in basalt short fiber content, especially for shorter exposure times. For long exposure times, however, this effect is less pronounced. The corrosion rate of the unreinforced matrix alloy is higher than those of the composites because in the former, there is no reinforcement phase and the matrix alloy does not have much corrosion resistance to the acid medium. In the present case, the corrosion rate of the composites as well as the matrix alloy is predominantly due to the formation of pits and cracks on the surface. In the case of base alloy, the strength of the acid used induces crack formation on the surface, which eventually leads to the formation of pits, thereby causing the loss of material. The presence of cracks and pits on the base alloy surface was observed clearly. Since there is no reinforcement provided in any form the base alloy fails to provide any sort of resistance to the acidic medium. Hence, the corrosion rate in the case of unreinforced alloy is higher than that in the case of composites. Basalt fiber, being the ceramic remains inert, is hardly affected by acidic medium during the test and is not expected to affect the corrosion mechanism of the composite.

It was observed that, in basalt short fiber reinforced aluminum composites, pitting depends on the local basalt short fiber distribution. Larger weight percentages of basalt short fiber could result in more opportunities for film disruption and more sites for pit initiation. The composites show the formation of pits on the surfaces, which is more with the increase in the percentage of basalt short fiber. Figure 2 shows the SEM micrograph exposing more pit formation of the matrix alloy and 10 wt% basalt short fiber reinforced composites than the matrix alloy. This is obviously due to the matrix/fiber interface which provides favorable sites for the formation of pits on the surface which lead to the removal of material, thereby leading to a weight loss. The corrosion result indicates a decrease in the corrosion rate as the percentage of basalt short fiber increases in the composite, which shows that the basalt short fiber, directly or indirectly, influences the corrosion property of the composites. Nevertheless, the results show a decrease in the corrosion rate as the basalt fiber content is increased in the composite, indicating that the basalt fiber does influence the corrosion characteristics of the composites. Sharma *et al.* [32] who obtained similar results in glass short fiber reinforced ZA-27 alloy composites reported that the corrosion rate decreases with the increase in the reinforcement. The glass fiber definitely plays a subsidiary role as physical barriers to the initiation and developed of pitting corrosion, modifying the microstructure of the matrix material, hence improving the corrosion. B. M. Sathish *et al.* [33], who obtained similar results in glass short fiber reinforced Al 7075 alloy composites, reported that the corrosion resistance increases with the increase in the reinforcement.

3.3. Microstructural Studies

Figure 2 shows the micrographs of the microstructure of the Al 7075 matrix as well as the composites examined by optical microscopy before performing corrosion test. As shown in figures, the basalt short fiber was successfully dispersed into the Al 7075 matrix. The micrographs indicated that the production of bulk MMCs using compocasting technique, used in the current study, is effective. The results of the microstructure analysis are shown in Figure (2a) in both longitudinal and transverse orientations, the Al 7075 alloy shows well defined, elongated grains. Figure (2b) shows a similar visible grain structure, but much of this long grain appears to be sheared into shorter section with a greater texture. The basalt short fiber distribution was observed and some pores were absorbed with 7.5 wt.% Al/basalt short fiber as shown in Figure (2c). The composite with 10 wt.% Al/basalt short fiber did not induce variations in the fiber size; the fiber distribution was fairly uniform in the composites as shown in Figure (2d).

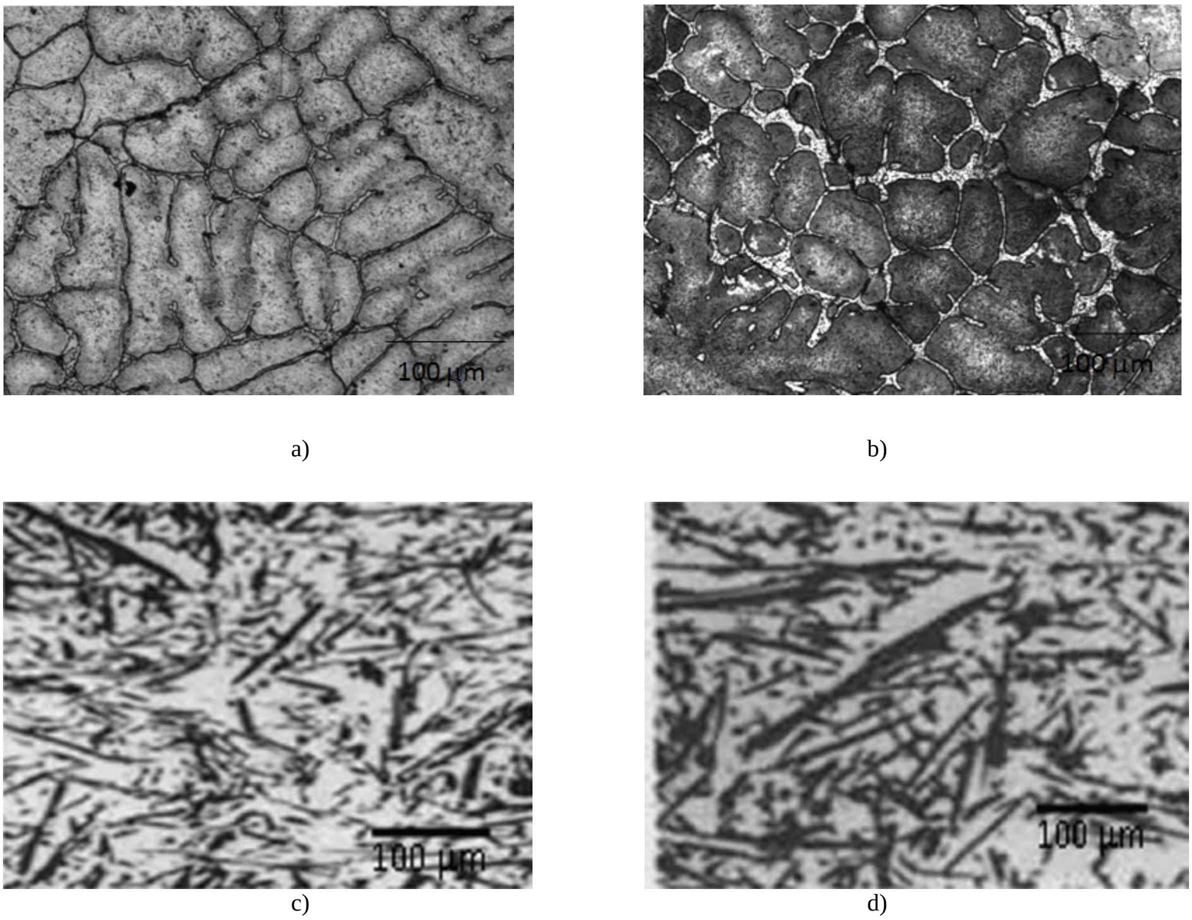

Figure 2. The microstructure of Al/ basalt short fiber composites containing a) 0 wt.%, b) 2.5 wt.%, c) 7.5 wt.%, d) 10 wt.% basalt short fiber.

3.4. Corrosion Morphology

Figure 3 shows a typical SEM of the unreinforced matrix alloy, revealing the presence of cracks on the surface. Pitting morphology was observed on the surface of the specimens after the tests. Small pits, not visible to the naked eye, were observed on specimens tested in acidic solutions. Inside these pits, the attack was selective along certain crystallographic directions. In the case of composites, intense localized attacks were seen at the fiber matrix interface. Pitting occurred preferentially in correspondence with basalt short fiber clusters. It gave rise to a few wide pits, which were distributed on the surface of the specimen. This was particularly evident by volcano-shaped pits appeared to be covered with white, thick, flaky corrosion product as it was in the case of 10 wt.% of basalt short fiber composites. These were seen to develop along the grain boundaries, and the crack size and depth increased with the addition of basalt fiber. The surface of the unreinforced matrix underwent a severe degradation, especially along the grain boundaries, providing preferential initiation site because of the discontinuity in the alloying elements due the changed substrate structures. Such a discontinuity would facilitate the passage of hydrogen ions to the metal, which once contacted by ions would suffer localized corrosion.

In the case of the composite containing 10% by weight of basalt short fiber, in addition to grain boundary attack, pitting occurred at the site of fiber dispersed in the matrix. The sizes of pits were seen to increase with the addition of basalt fiber. Pitting at the sites of the fiber dispersed in the matrix was found to be more dominant than the corrosion along grain boundaries. Studies of composites immersed for the prescribed periods clearly showed localized corrosion taking place at the fiber/matrix interface. Various researchers [34-36] found that MMCs show increased susceptibility to pitting attack when compared to non-reinforced alloys voids at the matrix/reinforcement interface. Surface and inter porosity of the composites tends to increase the interior exposing area of the specimens, which may increase the corrosion rate.

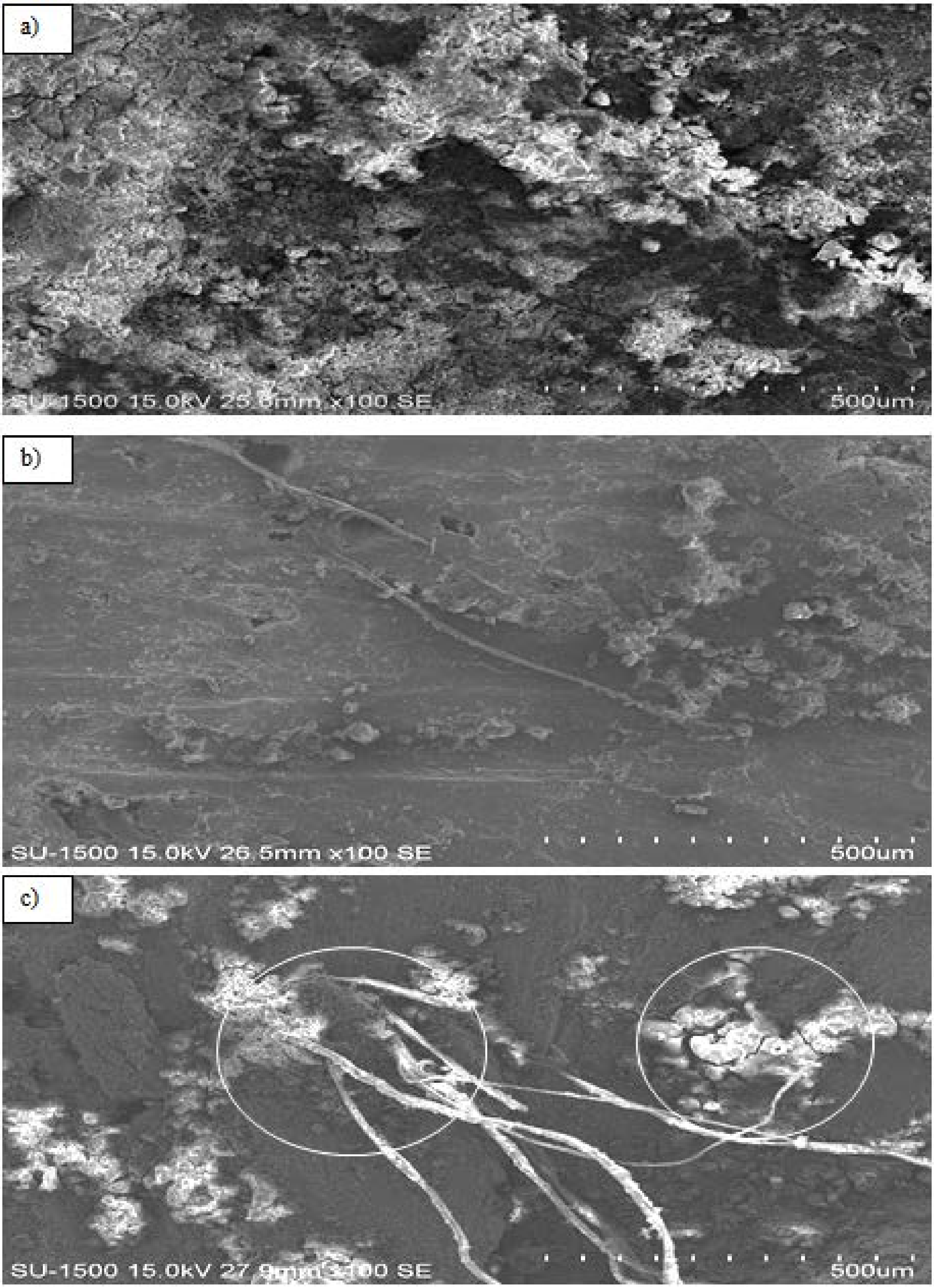

Figure 3. Shows corroded surface of the a) as cast Al7075 alloy, b) Al/ 5 wt. % of basalt short fiber and c) Al/ 10 wt.% of basalt short fiber composite

4. Conclusion

Based on the systematic study of the corrosion characteristics of Al/basalt short fiber the following conclusions are made:

- Al 7075/basalt short fiber MMCs were successfully fabricated using compo-casting method.
- Al 7075/basalt short fiber MMCs were found to corrode in 1M HCl solution.
- The corrosion rates of Al 7075/basalt short fiber MMCs as well as the matrix alloy were decreased with increasing exposure duration. However, increasing the weight percent of the basalt fiber tends to decrease the corrosion rate of the composite materials.

References

[1] P. J. Ward, H. V. Atkinson, P. R. G. Anderson, L. G. Elias, B. Garcia, L. Kahlen and J-M. Rodriguez-Ibabe, "Semi-solid processing of novel MMCs based on hypereutectic aluminium-basal short fiber alloys" Acta Materialia, Vol. 44 (1996), No. 5 , pp.1717-1727.

[2] C. M. Ward-Close, L. Chandrasekaran, J. G. Robertson, S. P. Godfrey and D. P. Murgatroyde, "Advances in the fabrication of titanium metal matrix composite", Materials Science and Engineering A, Vol. 263 (1999), No. 2, pp. 314-318.

[3] F. E. Kennedy, A. C. Balbahadur and D. S. Lashmore "The friction and wear of Cu-based basal short fiber carbide particulate metal matrix composites for brake applications", Wear, Vol. 203-204(1997), pp.715-721.

[4] H. Akbulut, M. Durman and F. Yilmaz, "Dry wear and friction properties of δ-Al_2O_3 short fiber reinforced Al-Si (LM 13) alloy metal matrix composites", Wear, Vol. 215(1998), No.1-2, pp.170-179.

[5] B.M.Girish et.al. "Fractography, Fluidity and tensile properties of aluminium/Haematite particle composite", Journal of Mateials Engineering and performance, Vol. 8 (1999), No. 3, pp. 309-314.

[6] B.M.Satish et.al. "Effect of short glass fibers on the mechanical properties of cast ZA-27 alloy composites", Material and Design, Vol. 17 (1996), No. 5/6, pp. 245-250.

[7] P.Reynaud "Cyclic fatigue ceramic-matrix composites at ambient and elevated temperatures". Composite Science and Technology, Vol.56, (1996), pp. 809-814.

[8] Zhang H, Zuo Y. The improvement of corrosion resistance of Ce conversion films on aluminum alloy by phosphate-treatment. Applied Surface Science Vol. 254 (2008), No. 16, pp. 4930-4935.

[9] L.A. Dobrza´nski, A. Włodarczyk, M. Adamiak, "Proceedings of the Powder Metallurgy World Congress and Exhibition", Vienna, 2004 (CD-ROM).

[10] L.A. Dobrza´nski, A. Włodarczyk, M. Adamiak, Proceedings of the 12th Scientific International Conference on Achievements in Mechanical and Materials Engineering (AMME'2003), Politechnika´ Slaska, Gliwice-Zakopane, 2003, pp. 297.

[11] Padro, A., Mercino, M.C., Viejo, F., "Influence of reinforcement proportion and matrix composition on pitting corrosion behavior of cast aluminium matrix composites". Corros. Sci. Vol.47 (2005), pp. 1750–1764.

[12] Oguzie, E.E., "Corrosion inhibition of aluminum in acidic and alkaline media by Sansevieria trisfasciata extract". Corros. Sci. Vol.49 (2007), pp. 1527–1539.

[13] Rehim, S.S.A., Hamdi, H.H., Mohammed, A.A., "Corrosion and corrosion inhibition of Al and some alloys in sulfate solutions containing halide ions investigated by an impedance technique". Appl. Surf. Sci. Vol. 187(2002), pp. 279–290.

[14] Salih, S., Juaid, A.I., "Mono azo dyes compounds as corrosion inhibitors for dissolution of aluminum in sodium hydroxide solutions". Portug. Electrochim. Act. Vol. 25 (2007), pp. 363–373.

[15] Satpati, A.K., Ravindran, P.V.,"Electrochemical study of the inhibition of corrosion of stainless steel by 1,2,3-benzotriazole in acidic media". Mat. Chem. Phys. Vol. 109 (2008), pp. 352–359.

[16] Bakkar, A., Neubert, V., "Corrosion characterization of alumina–magnesium metal matrix composites. Corros. Sci. Vol. 49 (2007), pp. 1110–1130.

[17] Brett, C.M.A., "On the electrochemical behaviour of aluminum in acidic chloride solution". Corros. Sci. Vol. 33 (1992), pp. 203–210.

[18] Candan, S., Biligic, E., "Corrosion behavior of Al–60 vol.% SiCp composites in NaCl solution". Mater. Lett. Vol.58 (2004), pp. 2787–2790.

[19] Daniela Alina Necşulescu "The effects of corrosion on the mechanical Properties of aluminium alloy 7075-T6, U.P.B. Sci. Bull., Series B, Vol. 73, Iss. 1, 2011.

[20] R. Karthigeyan, et al. "Mechanical Properties and Microstructure Studies of Aluminium (7075) Alloy Matrix Composite Reinforced with Short Basalt Fibre", European Journal of Scientific Research; Vol.68 (2012), No.4, pp. 606-615.

[21] S. Ezhil Vannan, S. Paul Vizhian "Statistical Investigation on Effect of Electroless Coating Parameters on Coating Morphology of Short Basalt Fiber" Jordan Journal of Mechanical and Industrial Engineering; Vol. 8 (2014), No. 3, pp. 153- 160.

[22] S. Ezhil Vannan, S. Paul Vizhian "Microstructure and Mechanical Properties of as Cast Aluminium Alloy 7075/Basalt Dispersed Metal Matrix Composites" Journal of Minerals and Materials Characterization and Engineering, Vol.7 (2014), No.2, pp.182-193.

[23] S. Ezhil Vannan, S. Paul Vizhian "Corrosion Behaviour of Short Basalt Fiber Reinforced with Al7075 Metal Matrix Composites in Sodium Chloride Alkaline Medium" J. Chem. Eng. Chem. Res., Vol. 1 (2014), No. 1, pp. 1-5.

[24] D. M. Aylor and P. J. Moran, "Effect of reinforcement on the pitting behavior of aluminum-base metal matrix composites," Journal of the Electrochemical Society, Vol. 132 (1985), No. 6, pp. 1277–1281.

[25] ASTM Standard, "Standard practice for laboratory immersion corrosion testing of metals," American Society for Testing and Materials G31-72, 2004.

[26] ASTM Standard, "Standard practice for preparing, cleaning, and evaluating corrosion test specimens," American Society for Testing and Materials G1-03, 2004.

[27] Weifeng Xu, Jinhe LIU, "Microstructure and pitting corrosion of friction stir welded joints in 2210-0 Aluminium alloy thick plate" Corrosion Science, Elsevier, Vol. 51(2009), pp.2743-275.

© 2015 Jordan Journal of Mechanical and Industrial Engineering. All rights reserved - Volume 9, Number 2 (ISSN 1995-6665)

[28] B. P. Bofardi, “Control of environmental variables in water reticulating systems,” in Metals Handbook, vol. 13 of Corrosion, p. 487, ASM International, Materials Park, Ohio, USA, 9th edition, 1987.

[29] L. H. Hihara and R. M. Latanision, “Suppressing galvanic corrosion in graphite/aluminum metal-matrix composites,”Corrosion Science, Vol. 34 (1993), No. 4, pp. 655–665.

[30] J.M.G.DeSalazar, A.Urefia, S.Mazanedo and M.Barrens "Corrosion behaviour of AA6061 and AA7075 reinforced with Al2O3 particulates in aerated 3.5% chloride solution potentiodynamic measurements and microstructure evaluation", Corrosion Science, Vol. 41 (1999), pp 529-545.

[31] J.E. Castle, L.Sun and H.yan,"The use of scanning auger microscopy to locate cathodic centers in SiC/Al6061 MMC And to determine the current density at which they operate" Corrosion Science, Vol. 36 (1994), No. 6, pp1093-1110

[32] S.C. Sharma “Aging characterstics of short glass fiber reinforced ZA-27 alloy composites materials”, Journal of material engineering and performance, Vol. 7 (1998), No. 6, pp.741-750.

[33] B.M. Satish et.al. "Corrosion characteristics of ZaA-27/glass-fiber composites", Corrosion science, Vol. 39 (1997), No. 12, pp 2143-2150.

[34] M. A. Afifi **“**Corrosion Behavior of Zinc-Graphite Metal Matrix Composite in 1M of HCl”, Hindawi, Vol. 2 (2014), pp 1-8.

[35] B. Thirumaran, S. Natarajan, S. P. Kumaresh “Corrosion behaviour of CNT reinforced AA 7075 nanocomposites” Advances in Materials, Vol. 2 (2013), No. 1, pp 1-5.

[36] P.D. Reena Kumari, Jagannath Nayak, A. Nityananda Shetty “Corrosion behavior of 6061/Al-15 Vol. pct. SiC(p) composite and the base alloy in sodium hydroxide solution” Arabian Journal of Chemistry, Vol.15 (2012), pp 1-10.